land

MDPI

Article

Micrometeorological and Hydraulic Properties of an Urban Green Space on a Warm Summer Day in a Mediterranean City (Attica–Greece)

Nikolaos D. Proutsos *, Alexandra D. Solomou, Michaela Petropoulou and Nikolaos E. Chatzipavlis

Institute of Mediterranean Forest Ecosystems-Hellenic Agricultural Organization "DEMETER", Terma Alkmanos, 11528 Athens, Greece
* Correspondence: np@fria.gr

Abstract: Urban Green Spaces (UGSs) are considered the most effective tool to mitigate Urban Heat Islands (UHIs). The optical properties of the materials and the vegetation types of the UGSs affect their surface temperatures, directly influencing their cooling ability. The hydraulic properties of urban soils are also affected by the vegetation coverage. The aim of this study is to investigate the temperature and reflected radiation (albedo) differences between UGS's elements, around noon on a warm summer day, in Greece. The results indicate that green elements have smaller surface temperatures and higher reflectance compared to the artificial or the dry bare soil, presenting differences with the direct air temperature (measured above the surfaces with unshielded thermometers) −5.5 °C (shrubs), −3.8 °C (grass), +7.8 °C or +8.7 °C (paved surfaces inside or outside the UGS), +10.8 °C (dry bare soil), +12.2 °C (concrete) and +12.5 °C (asphalt), and albedo values 0.14 (grass and shrubs), 0.15 (dry bare soil), 0.27 (concrete), 0.21 (asphalt) and 0.20 (paved surfaces). The tree shades also produce great surface differences. The unsaturated hydraulic conductivity of the urban soil is greater than the surfaces covered with grass compared to the shrub-covered or bare soil, presenting values of 27.6, 10.8 and 11.4 mm h^{-1}, respectively.

Keywords: urban heat island; urban climate; urban green spaces; optical properties; surface temperature; albedo; green infrastructure; LIFE GrIn project; Mediterranean city

Citation: Proutsos, N.D.; Solomou, A.D.; Petropoulou, M.; Chatzipavlis, N.E. Micrometeorological and Hydraulic Properties of an Urban Green Space on a Warm Summer Day in a Mediterranean City (Attica–Greece). *Land* **2022**, *11*, 2042. https://doi.org/10.3390/land11112042

Academic Editors: Giulia Capotorti and Simone Valeri

Received: 23 October 2022
Accepted: 11 November 2022
Published: 14 November 2022

1. Introduction

Urban Green Spaces (UGSs) provide multiple benefits for local communities [1]. Their importance has been enhanced and acknowledged by the public, especially during the last decades, mainly due to the expanding urbanization and, most recently, due to the restrictions imposed by the spread of the COVID-19 pandemic [2]. The most important benefit of urban vegetation is its ability to regulate urban climate by affecting several micrometeorological attributes of the urban environment that impact the exchange of the mass and energy fluxes, providing a cooling effect and relieving the impacts of the Urban Heat Island (UHI) phenomenon.

The characteristics of the UGS and the persisting weather conditions in each area can highly affect its ability to regulate urban climate. The seasonal radiation conditions and the size of the park are among the more influential parameters for the parks' cooling effect [3], whereas the shape of the green area, its coverage with trees and shrubs and grass-covered surfaces also affect UGSs' cooling effects [3]. Following up on the findings of other studies [4–8], it is concluded that the proportion of green areas within an urban setting is a key role factor in the distribution of the UHI intensity. According to Qui et al. [9], the intensity of the UHI phenomenon can be relieved by up to 1.57 °C in comparison with surrounding commercial areas, addressing evapotranspiration as an efficient attrib-

ute for UHI mitigation. Maimaitiyiming et al. [10] also suggest that the presence of vegetated areas lowers local temperatures, underling the importance of the quality characteristics of the green areas, i.e., the density of green patches might be positively linked with alleviation of the UHI but cannot compare in strength with the cooling effect that an uninterrupted large green space would offer, a fact also pointed out by Cao et al. [3], Li et al. [11] and Zhang et al. [12]. Qui et al. [13] reported that urban vegetation could amount to a 0.5–4.0 °C reduction in the air temperature of the neighboring area, whereas Mackey et al. [14] suggest that an NDVI (index indicative of vegetation cover) above 0.35 triggers a notable temperature drop. Jusuf et al. [15] observed a considerable correlation between land use and temperature data, as well as an obvious temperature reduction as the vegetation body increased. Similarly, Huang et al. [16] studied the cooling effects of several UGSs across Harbin, China, factoring in the features of the parks, and determined that the vegetal arrangement, including the size and shape of the parks, is positively linked to their cooling efficiency. They confirmed, using the NDVI, that higher vegetation cover translates into a less intense UHI phenomenon, a point also supported by Bao et al. [17].

Edmondson et al. [18] identified an alleviating effect of the UHI by vegetation cover, distinguishing the higher potential of woody plants compared to herbaceous coverage. They noted that the mean maximum surface temperature of the soil was mediated by about 5.7 °C more by the presence of trees and scrubs when compared to the effect of grass-covered surfaces. During summer, the estimated residual temperature under tree cover was found to be negative, whereas it was found to be positive in the case of non-woody coverage, and this relationship seems to be reversed in winter. However, they noted that, as also reported by Armson et al. [19] and Wu et al. [20], the existence of trees in urban environments, while it might offer benefits due to shading, can also hinder the free movement of air currents, thus impeding the release of long-wave radiation at nighttime, trapping heat.

The use of different materials in the city and also inside the UGSs may also affect their energy exchange characteristics. Mohajerani et al.'s [21] research on the contribution of different materials used in urban areas to the UHI phenomenon revealed asphalt's and concrete's great significance since their presence basically boosts the UHI. They note that asphalt's high heat capacity and low albedo in combination with its extensive use in cities largely influence the urban environment's thermal conditions. It has been reported that freshly paved asphalt concrete can capture up to 95% of the received solar radiation [22] thus easily surpassing surface temperatures of 60 °C on hot summer days. As commented by Grimmond [23], the artificial materials commonly used in urban surfaces differ substantially in their thermal, hydraulic and radiative properties from naturally occurring ones. They also state that modifying the albedo of a surface is an easier and more tangible solution than meddling with any of its other characteristics to mitigate UHI and that a suggested practice is to add a top, light-colored, low-albedo layer on paved surfaces to enhance its reflectance and promote the return of radiation back to the atmosphere.

Generally, solar radiation drives plants' physiological processes and productivity [24]. Solar light availability, especially at the photosynthetically active waveband [25–27], in conjunction with the plant's optical properties (reflectance, transmittance and absorbance), determines the energy and mass fluxes of the vegetation-covered surfaces and ecosystems [28]. The radiation reflectance of urban surfaces is considered a most influential factor for UHI [29]. The surfaces that comprise urban landscapes have lower reflectivity, larger heat capacity, and generally different thermal properties than others in less built-up areas, thus storing more solar energy, which, in turn, translates into higher surface temperatures [30,31]. Due to their high thermal inertia and heat flux, the surface materials that are commonly used in cities are greatly influenced by ambient temperatures [32]. In addition, the densely built space of the city does not allow the dispersal of long-wave radiation from the ground, effectively obstructing the otherwise naturally occurring reduction in temperature [33–35]. Baldinelli et al. [29] suggest that an increase in radiation reflectance in the city (urban albedo) would result in its cooling. Similarly, Erell et al. [36]

state that the high albedo surfaces result in lowering air temperature but increase the thermal stress in sunny conditions due to radiant exchange.

Most studies conducted in cities analyze the impacts of UGSs on UHI by assessing differences in air temperature between highly built-up and open, green or not, spaces. Specifically for Athens—Greece, Giannopoulou et al. [37] identified five geographic zones in the city with different thermal balances. The authors explored the heat island phenomenon in 25 sites in Athens during the summer season and found higher air temperatures in the industrial western part and in the center of the city and lower in its northern and eastern parts. Their findings are in line with those by Livada et al. [38], who also mention that UHI was developed intensively in the central and western industrialized part of the city.

Skoulika et al. [39] studied the cooling island intensity of an urban park in Athens during summer and confirmed its important mitigation impact on its surroundings, whereas Zulia et al. [40] investigated the microclimatic conditions in the National Garden in the center of Athens during summer and found a clear influence of the park, being cooler compared to other monitored urban locations, with greater air temperature differences during the night in streets with high buildings and wide streets with low traffic, whereas the relative differences were higher during the daytime in streets with high anthropogenic heat during the day.

Melas et al. [41] examined the microclimatic conditions of small open spaces (small courtyards and backyards) and found that vegetated backyards produce stronger cool island patterns compared to non-vegetated spaces. Tsiros and Hoffman [42] also evaluated the cooling effect in a courtyard's garden during a hot weather summer period in Athens and found a well-defined and strong daytime cool island and a significant air temperature reduction compared to an urban square with low canopy coverage. In addition, Tsiros [43] studied the trees cooling effect in Athens by measuring air temperature under the canopy in five streets during the exceptionally hot weather period in 2007 and found that the trees' average cooling effect at noon varied from 0.5 to 1.6 °C.

UGSs also provide important services for flood prevention due to the high water absorption by the soil, which is highly affected by the type of urban vegetation cover. Hidayat et al. [44] mention that soil characteristics including hydraulic conductivity are affected by the forest canopy cover, with higher hydraulic conductivity and thus infiltration rate at high-density canopies. Luo et al. [45] reported the different hydraulic profiles of clay soils covered by different vegetation types or with no coverage. Measurements of the unsaturated hydraulic conductivity showed that planting Vetiver grass causes a significant rise in hydraulic conductivity values, probably due to the structure of its root system, whereas, conversely, the Bermuda grass cover reduced the conductivity compared to the reference bare soil studied. The same pattern was observed when it comes to the infiltration rate, with the Vetiver grass almost doubling its value, whereas the Bermuda grass cut it in half. Gadi et al. [46] inquired into the variation in the hydraulic properties of the soil in close proximity to a tree, taking into account the state of vegetation cover. When studying the hydraulic conductivity as a function of floral density, they discovered that densely vegetated soils differed by 33–99% from soils with poor vegetation cover. This can be attributed to the intensified suction related to the water uptake by roots, which in turn lessens the water flow through the soil [47,48]. Multiple studies have showcased the escalation potential of hydraulic conductivity as a response to the growth of the plant's root system [49–51], which is accredited to water's preferential flow around the roots [52]. Gadi et al. [46] also marked the significant influence of the presence of shredded leaves upon the soil surface, as the associated hydraulic conductivity was 49–100% higher than in portions where leaves were absent. Jarvis et al. [53] studied the effects of both land use and climate on the hydraulic conductivity values and found that arable sites have, on average, ca. 2–3 times smaller saturated water conductivity than natural vegetation, forests and perennial agriculture.

Galli et al. [54] measured the unsaturated hydraulic conductivity in degraded and rehabilitated urban green spaces and found increased values in rehabilitated soils, especially five years after the soil rehabilitation process. They also concluded that in spaces with an absence of soil and vegetation maintenance, the unsaturated hydraulic conductivity may decrease after 9–12 years. Vegetation improves the soil structure and increases the soil's unsaturated conductivity. In addition, Galli et al. [54] identified the time since soil rehabilitation, the soil compaction and the vegetation cover as the most critical factors affecting the unsaturated hydraulic conductivity. They suggested that the higher unsaturated hydraulic conductivity values in the examined rehabilitated green spaces are associated with the time after the vegetation introduction and the development of the plant's root system and the development of a coherent soil matrix with stable connections between pores and the establishment of pathways for the water movement.

Based on the above findings, it is concluded that the optical properties of the UGSs determine the microclimate of a city. Along with the UGSs' soil characteristics, the basic cycles of energy and water in the city are highly affected, impacting also the quality of life of the citizens. The aim of this study is to investigate the differences in the surface temperatures of the green and grey elements inside an urban park and extend our knowledge on the performance of UGSs on absorbing/reflecting radiant energy and infiltrating water, under the weather conditions persisting in a hot summer day at a city with a Mediterranean climate.

2. Materials and Methods

This work was implemented for the broader area of Athens (Attica) in the Municipality of Amaroussion. The long-term meteorological data for the region, derived by the nearest station of N. Philadelphia (38.05° N, 23.67° E, alt.: 12 m, operated by the Hellenic National Meteorological Service) indicate that the climate is semi-arid, according to UNEP's [55] aridity climate classification, which is based on Thornthwaite's [56,57] water balance approach, with an aridity index value of 0.44 for the period 1955–2019 [58,59], presenting a decadal trend to more arid conditions [60].

The study site is an urban green space (38.04° N, 23.80° E, alt.: 190 m), with a total area of 0.91 ha covered by different types of materials including both green (trees, shrubs and grass) and grey (paved corridors and concrete) elements, whereas the UGS is surrounded by asphalt roads (Figure 1).

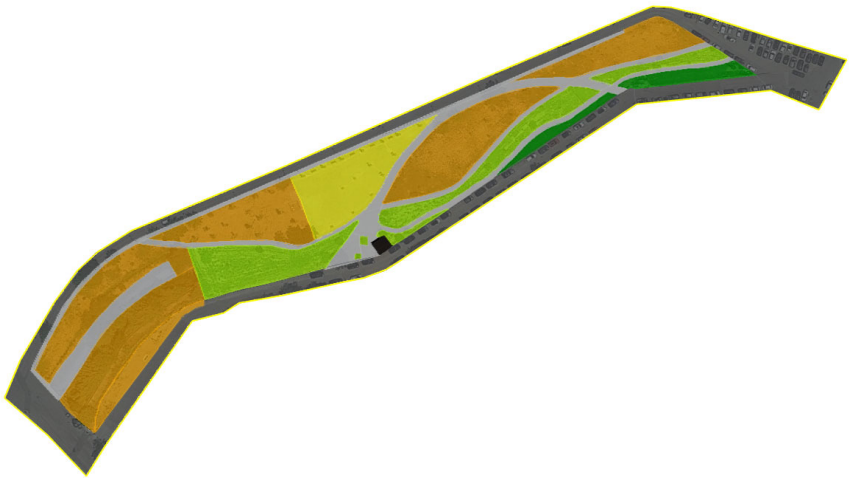

Figure 1. Different types of land cover (materials) in the UGS, i.e., asphalt (dark grey), paved surfaces (light grey), concrete (yellow), non-irrigated soil with trees (orange), shrubs (light green) and grass (dark green) (base map by Google Earth, Image © 2022, Google, Maxar Technologies).

The vegetation in the UGS includes trees, shrubs and herbaceous plants. The trees are generally deciduous broad-leaved (e.g., *Tilia tomentosa*, *Acer negundo*, *Melia azedarach*,

Platanus orientalis, *Morus alba*, *Cercis siliquastrum*, *Prunus cerasifera*, *Ailanthus altissima*) and randomly distributed in the UGS. Most of them are of small age (less than 5 years) and have not yet produced large canopies. The shrub-covered surfaces (Figure 1) host a variety of species (e.g., *Nerium oleander*, *Teucrium fruticans*, *Rosmarinus officinalis*, *Lavandula angustifolia*) in mixed patterns with herbaceous plants (e.g., *Calendula arvensis*, *Lactuca serriola*, *Matricaria recutita*, *Pallenis spinosa*, *Capsella bursa-pastoris*, *Solanum elaeagnifolium*, *Plantago lanceolata*, *Convolvulus arvensis*), whereas two surfaces were covered with grass (e.g., *Lolium perenne*, *Poa annua*, *Arundo donax*, *Cynodon dactylon*, *Eleusine indica*).

To study the micrometeorological environment inside the UGS, an automatic meteorological station was installed in 2019 by the Institute of Mediterranean Forest Ecosystems (IMFE), measuring several attributes including air temperature (at a height of 2 m above ground) and radiation attributes. For the study of the spatial variations in air and surface temperatures, portable sensors were used in order to take 258 point measurements at different points inside and outside the UGS. All measurements were taken during midday (from 13:00 to 15:00) of a hot summer day (23 June 2022) under clear sky conditions. A portable LP 471 RAD probe (Delta OHM), irradiance meter with cosine correction was used to measure shortwave solar radiation incoming and reflected flux densities within the spectral range of 400 to 1050 nm. In addition, an MI-210 infrared radiometer (Apogee Electronics) was used to measure surface temperatures above the different surfaces. The recordings of the surface temperatures were obtained by placing the sensor 40 cm above the surface facing downwards (zero angle). At the same height above the surfaces, the direct air temperature was measured with an HD 2301.0 handheld thermo-hygrometer (portable device with a Pt100 humidity/temperature combined sensor), considering that the substrate surface highly affects its above-measured air temperature [61] and thus the recordings of the portable device are more reliable compared to the temperatures recorded at the nearby meteorological station by a radiation-shielded thermometer. The sensor was directly exposed to radiation. To compare the differences in air temperature inside and outside the UGS, continuous 10-minute temperature and relative humidity data, along with global solar radiation flux densities, were obtained by both IMFE's station and a nearby (270 m distance) automatic meteorological station (model: Davis Vantage Pro 2 Plus) installed by the Municipality of Amaroussion, on the roof of a one-floor (with height about 5 m) elementary school building.

The ability of the UGS to infiltrate water was assessed by measuring the unsaturated hydraulic conductivity at specific points inside the UGS, covered with bare soil, shrubs and grass (Figure 2). The field experiments were conducted with a minidisk infiltrometer (Meter Group) and the unsaturated hydraulic conductivity was estimated according to the method proposed by Zhang [62], applying the van Genuchten parameters obtained from Carsel and Parrish [63]. Before each infiltration experiment, the soil moisture was measured with a delta-t, SM150 sensor. In total, nine infiltration experiments were conducted above bare soil, shrub-covered and grass-covered surfaces.

Zhang's [62] method is simple and reliable for measuring infiltration into dry soils. It uses cumulative infiltration (I) measurements plotted against time (t), and the results are fitted to the equation

$$I = C_1 \sqrt{t} + C_2 t \quad (1)$$

where C_1 and C_2 (in mm s^{-1}) are factors related to soil sorptivity and hydraulic conductivity, respectively.

The soil hydraulic conductivity (K) is estimated by the equation:

$$K = \frac{C_1}{A} \quad (2)$$

where A is an estimator calculated by the following equation:

$$A = \begin{cases} \dfrac{11.65\,(n^{0.1}-1)\,e^{2.92\ (n-1.9)\,a\,h_0}}{(a\,r_0)^{0.91}}, & for\ n \geq 1.9 \\ \dfrac{11.65\,(n^{0.1}-1)\,e^{7.5\ (n-1.9)\,a\,h_0}}{(a\,r_0)^{0.91}}, & for\ n < 1.9 \end{cases} \quad (3)$$

where n and a are the van Genuchten parameters that differ for specific soils [62], r_0 is the infiltometer's disk radius, and h_0 is the suction applied at the disk's surface. In our experiments, the soil was loamy sand, r_0 = 2.25 cm and h_0 = −1 cm.

In the present study, spatial patterns of the attributes measured or calculated in the UGS were also produced in the form of contour maps, by using the Surfer® ver. 13 Software [64]. Point Kriging geostatistical gridding method was applied to each irregularly spaced point dataset to produce accurate grid values. The method is widely used and reliable, estimating the unknown grid values at all points across a well-defined spatial domain by using weighted averages of all known values around each grid point [65].

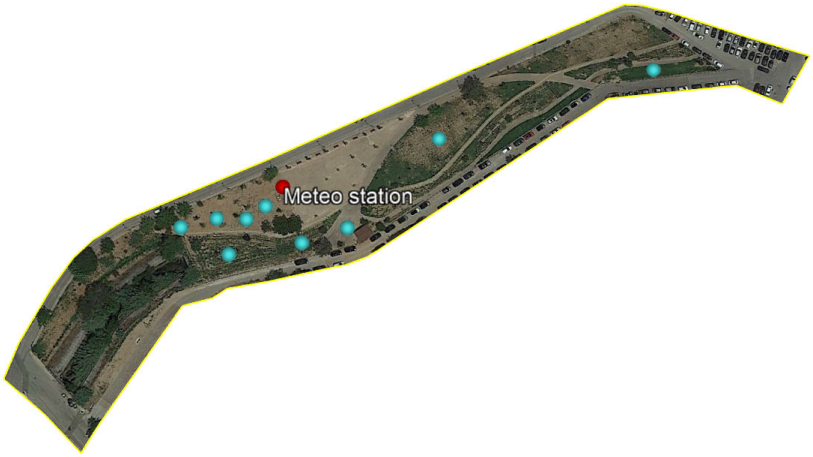

Figure 2. Points inside the UGS where infiltration measurements were taken for the estimation of the unsaturated hydraulic conductivity of the soil (4 points for dry bare soil, 3 points for shrubs and 1 point for grass) (base map by Google Earth, Image © 2022, Google, Maxar Technologies).

3. Results and Discussion

3.1. Temperature Attributes

During the warm summer day (23 June 2022) when measurements were taken, the air temperature inside the UGS was elevated, presenting a 24 h average value of 30.1 °C, which reached 36.0 °C at midday (13:00–15:00 h), whereas the soil temperature at 10 cm depth was even higher with a 24 h average 36.4 °C reaching 44.6 °C at midday (13:00–15:00 h). The respective air temperatures recorded on the concrete roof of the nearby building were similar and slightly higher (24 h average 30.3 °C and midday average at 13:00–15:00 h 36.3 °C). The 24 h temperatures were higher compared to the month's (June 2022) average by about 3.7 °C for air temperature and 2.8 °C for soil temperature in the UGS and by 4.2 °C for air temperature on the building's roof, indicating the hot conditions prevailing during the day when the measurement campaign was conducted.

The diurnal changes of the meteorological parameters during 23 June 2022 as recorded by both stations (inside the UGS and at the building's roof) along with the respective monthly average values for an average day of June 2022 are depicted in Figure 3. The air temperature and relative humidity in both stations appear to have similar values both during the day of the campaign (UGS 0.1 °C cooler than the roof) and during June 2022 (zero difference), especially during daytime (6:00–20:00 h). It is notable, however, that during the nighttime the temperature differences between the vegetation-covered UGS and the concrete-covered building's roof are maximized indicating cooler conditions in

the UGS by about −0.9 °C in June 2022 becoming higher (−2.0 °C) during the campaign's day. The pattern of the relative humidity is the opposite compared to the respective one of temperature, presenting similar values for both stations at daytime and higher values (+2.4% in June 2022 and +6.4% on 23 June 2022) at nighttime.

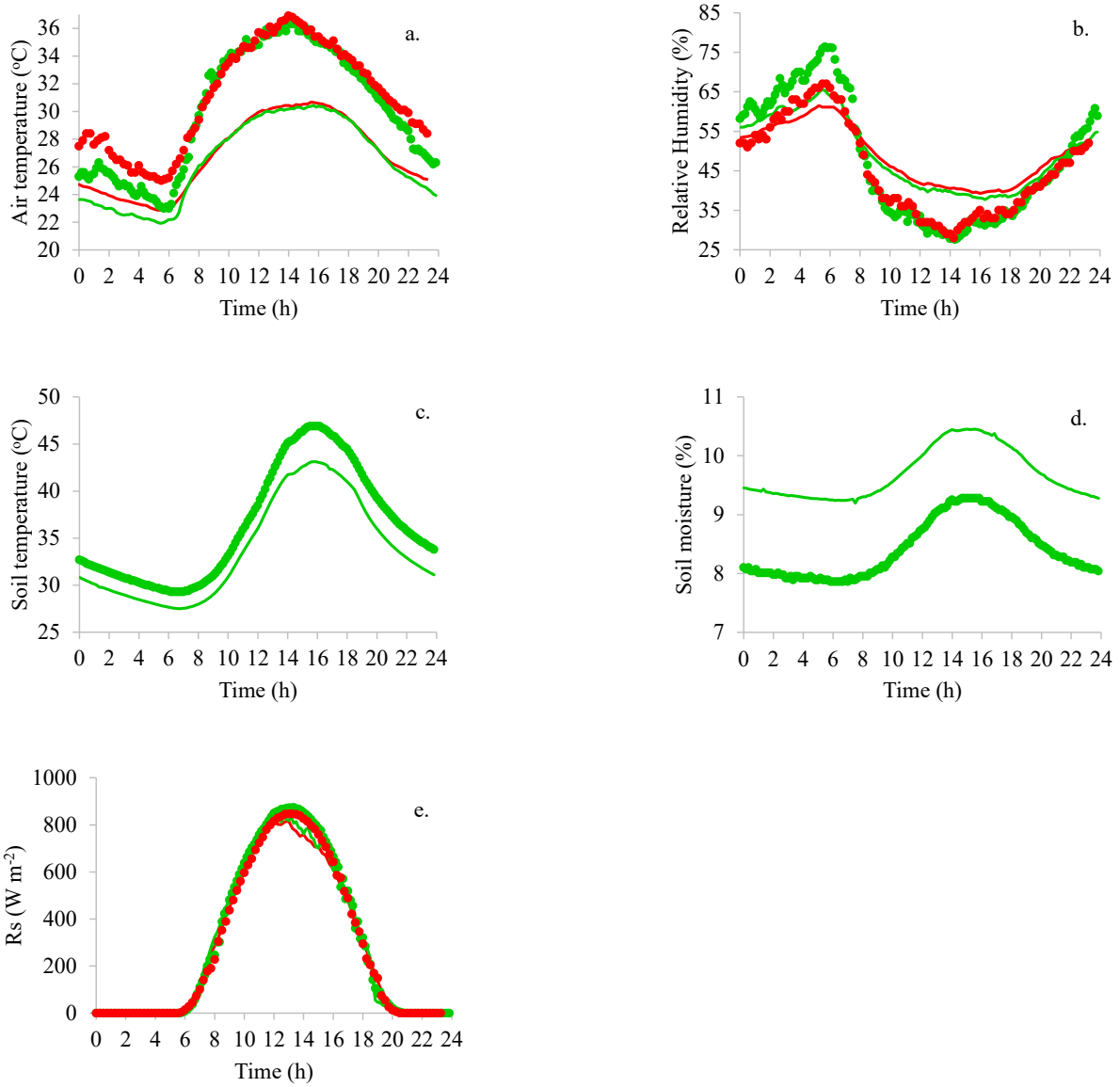

Figure 3. Average 10 min values of micrometeorological parameters: (**a**). air temperature, (**b**). relative humidity, (**c**). soil temperature, (**d**). soil moisture, (**e**). global solar radiation) measured inside the UGS (green) and on a nearby (270 m distance) roof of a building (red), during a warm summer day (23 June 2022, dots) and in all June 2022 (lines) in Amaroussion UGS.

Based on the above, the cooling effect of the UGS can be considered minor. However, this should be assessed in conjunction with the prevailing micrometeorological conditions during the very warm campaign day. The increased air temperature during the specific day, which reached 30.1 °C (compared to 26.4 °C for the average day of June 2022), presenting a maximum of 36.4 °C in association with the rather low relative humidity (daily average of 47.6% with a minimum 10 min value 27.6%), the cloudless sky conditions along with the high solar radiation flux density (24 h average 300.0 W m^{-2}, with maximum 10 min value 874.3 W m^{-2}) and the very high soil temperatures (daily average 36.2 °C with

maximum 10 min value 46.9 °C), impose a very high water demand for the vegetation to sustain high growth rates. Such conditions, considering also the extremely reduced water availability in the rootzone (soil moisture 8.4% p.v.), define the reduced evapotranspiration rates and, thus, the less effective cooling ability of the plants to allocate water and energy from soil to the atmosphere. For the specific UGS, the municipality green managers apply deficit irrigation in an attempt to reduce water consumption, and this decreases the UGS's ability to produce cooling benefits to a maximum degree. The issue of reducing water consumption in UGSs, through plant selection or deficit irrigation, is critical and rather complicated, especially in the Mediterranean region, where water scarcity, on one hand, and the increased impact of UHI, on the other, impose contradicting criteria for UGS's design and management. The cooling effect is also associated with the size of the UGS, its shape and the vegetation architecture, which, in our case, consists of young trees with no fully developed canopies that enhance the openness of the park, resulting in a negative effect on the air temperature [66]. According to Jaganmohan et al. [67], the larger the area of an UGS, the more prominent the associated cooling, though manifested differently depending on the landscape type (forests vs. parks). In their research on several UGSs in Leipzig Germany, it was also indicated that the shape factor also affects their cooling ability. Moreover, the features of the green space are more significant than those of their surroundings when it comes to the UGS's cooling efficiency. Similarly, Monteiro et al. [68] assessed various sized UGSs in London, observing that very small UGSs (less than 0.8 ha) had no discernable cooling effect beyond their boundaries, but sizing up, one can note the drop in the air temperature of the surrounding environment. Furthermore, the tree canopy cover proved to be positively related to the cooling distance, but the degree of cooling was more strongly linked to the grass cover of the green space.

The general effect of the UGS was further assessed by analyzing surface temperature data taken above surfaces covered with different green and grey materials inside the park. The spatial patterns produced by the instant air temperature and surface temperature values in the UGS, after applying Kriging's interpolation, are depicted in Figure 4. The surface temperatures measured at several points of the UGS during midday (13:00–15:00) were, in general, higher for the artificial surfaces compared to the ones covered with natural elements. More specifically, surface temperatures above asphalt during midday were the highest, compared to all other materials, reaching an average of 54.4 °C, and were about +12.5 °C warmer compared to the direct air temperature measured just above the surface. The respective differences with the air and soil temperatures obtained by the meteorological station were even higher (18.2 and 8.4 °C, respectively). Similar was the behavior of the concrete-covered surface inside the park, which presented an average surface temperature of 52.9 °C, +12.8 °C higher than the above-point-measured direct air temperature, being +18.0 °C and +11.94 °C warmer than the air and soil temperatures measured by the meteo station, respectively. The internal paved corridors inside the UGS also presented high surface temperatures (average 51.4 °C) and they were also higher compared to the direct air temperatures above their surfaces (+8.7 °C), and much higher compared to the air and soil temperatures measured by the meteo station (15.2 and +5.4 °C, respectively). The respective temperature differences of the paved surfaces surrounding the UGS were also of the same magnitude since their average surface temperature was 49.6 °C, about +7.8, +13.8 and +3.3 °C warmer than the direct air temperature above the surfaces and the air or soil temperatures of the station inside the UGS, respectively. The above pattern is rather expected since the artificial elements absorb the radiant energy from the sun and store it in the form of heat, increasing their temperature.

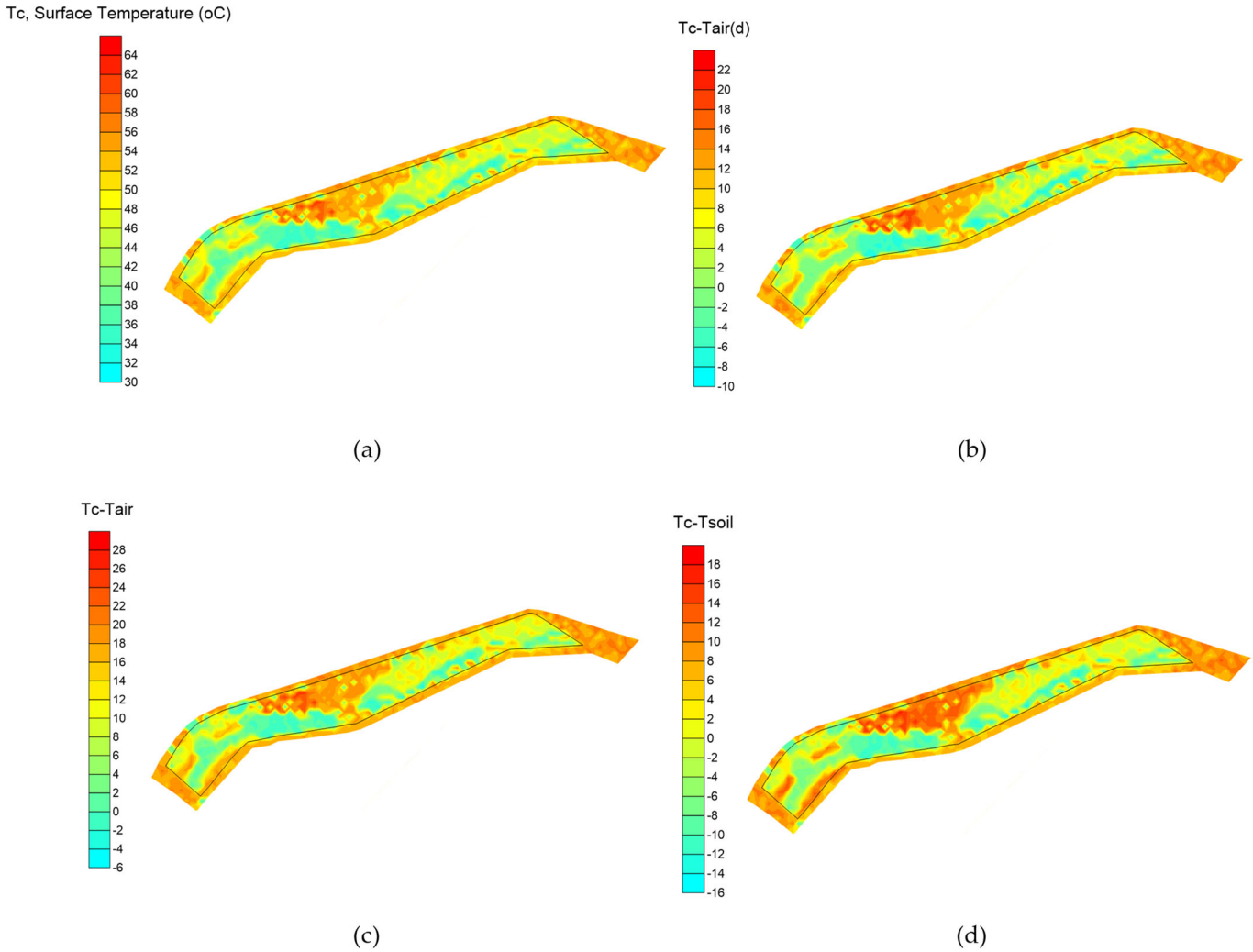

Figure 4. Spatial changes in (**a**) surface temperature in the UGS and differences (**b**) with direct air temperature measured above each point with sensor without radiation shield (**c**) with air temperature derived from the stationary meteorological station and (**d**) with soil temperature.

The general pattern of the above-mentioned artificial surfaces, appears to be followed in the case of dry bare soil, which also presents high surface temperatures of the same magnitude (average 50.0 °C) during the hot summer midday, being +10.8 °C warmer compared to the direct air temperatures above the surface and +15.9 and +6.6 °C warmer than the air and soil temperatures of the station inside the UGS. This is also expected since the dry and non-vegetation-covered (bare) soil appears to behave as an artificial material, storing heat and increasing its temperature.

The effect of the live vegetation tissues is quite different since the absorbed solar energy does not transform into heat storage but is rather used to enhance the photosynthesis process. In our study, this seems to be true even under low soil water availability conditions. The natural surfaces covered with vegetation have lower surface temperatures compared to the artificial or dry bare soil-covered ones. More specifically, the surface temperature of the grass was measured on average to be 38.0 °C, i.e., −3.7 °C cooler compared to the direct temperature of the above air, −8.2 °C cooler than the soil temperature, but +2.2 °C warmer than the air temperature of the station inside the UGS.

The cooling effect of shrubs was even more evident. Their surface temperatures were the lowest recorded (average 36.8 °C), and they were −5.5 °C cooler compared to the direct air temperatures above the surfaces, −0.2 °C cooler compared to the air temperature of the station and −9.9 °C lower than the soil temperature.

It should be noted that the above patterns describe the behavior of the natural and artificial elements of the UGS during the summer Mediterranean noon on a very warm day and under conditions of limited soil water availability. This is expected to have reduced the cooling effect of the vegetation elements of the UGS, since only small water quantities would have been available to the plants for evapotranspiration in order to regulate their tissues temperatures and perform photosynthesis, considering that evapotranspiration is demonstrated to be the most effective way to improve UHI [9,69–71].

According to the results of the study of Đekić et al. [72], a distinct variation between the temperatures of various surfaces in UGSs was identified, particularly in the high solar radiation hours—around noon. More specifically, they found that the temperature difference between the grass surface (coolest) and the dark asphalt varied between 9 and 19.7 °C, whereas in our study it was on average 16.3 °C. In addition, Đekić et al. [72] also observed a difference of 10–24.5 °C between the hottest surface temperature and that of the ambient air, a range that is in line with the findings of our study where the respective difference between the asphalt and the ambient air temperature, measured by the meteorological station, was 18.2 °C. Similarly, Đekić et al. [72] mention that for the hotter period of measurements (mid-July to mid-August) the average maximum temperature for all artificial surfaces was well above 50 °C (average 52.1 °C in our study for all artificial materials ranging from 49.6 °C for the internal paved corridors to 54.4 °C for asphalt), while the grass-covered area more or less matched the temperature of the ambient environment, which is also in line with our study, since the temperature differences of grass and shrubs against ambient air temperature measured by our station were very close (38.0–35.8 °C and 36.7–36.1 °C, respectively.

During the measurement campaign, surface temperatures were also measured at shaded surfaces (below the tree canopies), to quantify how tree shades can reduce the increase in surface temperatures, especially above warm artificial surfaces and bare dry soil (Figure 4). The results indicate a rapid decrease in the surface temperature under shade in all cases. More specifically, the shaded asphalt was found to be –17.8 °C cooler than the unshaded, whereas similar differences were detected for the other surfaces (–15.2 °C for the internal paved corridors of the UGS, –11.6 °C for the concrete and −11.5 °C for the dry bare soil). The positive effect of shading is also portrayed by Đekić et al. [71] whereby even partly shaded asphalt surfaces were found to maintain lower temperatures than their counterparts that were fully exposed to sunlight.

3.2. Radiation Reflectance (Albedo)

The radiation reflectance of urban surfaces is considered the most influential factor for the Urban Heat Island effect [29]. The reflectance of the surfaces can highly affect their radiation budget and the radiative energy partitioning and exchange. The part of the incoming solar energy absorbed by the surfaces is determined by their reflectance characteristics including surface roughness and color. The shortwave radiation reflectance of a surface is the ratio of the reflected to the incoming global solar radiation flux density, and is commonly known as albedo.

The albedo changes above the different materials of the UGS of Amaroussion are depicted in Figure 5. Inside the UGS, the natural surfaces present, in general, lower reflectivity compared to the artificial surfaces, suggesting that they absorb more solar radiative energy. Specifically, the vegetation-covered surfaces, either with grass or shrubs, present albedos of about 0.14 and the dry bare soil appears to be of the same magnitude (0.15). On the other hand, the artificial surfaces' albedo is greater, being 0.27 for concrete, 0.21 for asphalt and 0.20 for the internal UGS's paved corridors.

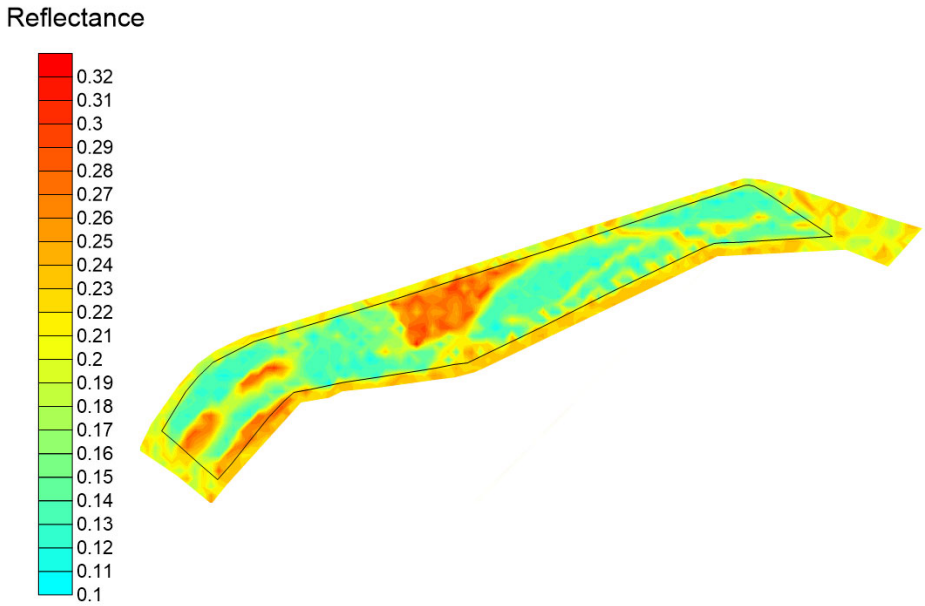

Figure 5. Spatial changes in the reflectance coefficient of shortwave solar radiation (albedo) inside the UGS.

Đekić et al. [72] cited the albedo values of some common urban artificial surfaces as well as those of green areas in order to accentuate their different influences on the city's thermal balance. Thereby, the albedo values' span for asphalt is 0.04–0.15 and the respective range for concrete is 0.10–0.35. As for the materials used for pedestrian routes, dark concrete tiles hold an albedo of 0.05–0.35 while white concrete tiles' albedo is considered to be around 0.70. Lawns and arbors have values of 0.25–0.30 and 0.15–0.18, respectively. Compared to our study, the values for asphalt and grass are quite different probably due to the different types of materials in the studies; however, the albedos of the other attributes are in line with our findings.

In general, high reflectance materials are suggested for use in UGS and cities in order to reduce radiation absorption and, thus, to prevent increasing surface temperatures, and they are considered as a cooling strategy to mitigate the UHI effect in cities [29]. It should be noted, however, that the reflected radiation in densely built cities with tall buildings is only partly reflected back to the atmosphere, mainly due to multiple radiation reflection and scattering between the surfaces, which finally trap the shortwave radiation in the building canopies, resulting in decreased urban albedo in the large scale of a city [73] with regard to the geometric structure of the buildings [74] and the scarcity of urban vegetation [75].

The reflectance of the materials inside the UGS differs at larger scales. Sugawara and Takamura [75] used radiometers to measure the surface albedo above two cities in Japan using a helicopter and found an albedo value of 0.12, whereas, in the nearby forest, it was higher (0.16). According to the authors, the lower city albedo is attributed to the roughness of the urban surface, which is enhanced by the city buildings and an increase in the absorbance of the urban surface. This appears to be contradicted when studying the optical properties of specific artificial materials since their surfaces are far smoother compared to the large scale of a city.

The part of the absorbed radiation by the artificial surfaces results in their temperature increase. In the case of the green elements, the absorbed radiation is mainly used for photosynthetic processes and, to a lesser degree, results in the increase in the tissues' temperatures. In our case, the lower reflectance of vegetation-covered surfaces results in greater sums of radiation absorbed by plants but, as already presented above, this did not lead to an increase in their temperature. It is worth noting that even the behavior of the

dry bare soil is similar to the plant-covered surfaces, as regards its optical characteristics, but this increased radiation absorbance increased the heat storage in the soil, resulting in its higher temperatures.

3.3. Soil Water Infiltration

Water infiltration ability is a significant parameter in soil research and an important attribute for the UGSs, indicating the ability of the soil to absorb water. The unsaturated hydraulic conductivity is a measure of this soil's ability, highly associated with the specific soil mechanical characteristics and especially the coverage of its upper layer. In the UGS of the present study, nine infiltration experiments were conducted at different points in the UGS covered with shrubs, grass and dry bare soil. The results of the analysis are depicted in Figure 6, indicating that grass-covered surfaces present a higher ability to infiltrate water compared to dry bare soil and shrub-covered surfaces. The respective average unsaturated hydraulic conductivity values are 27.6 mm h^{-1} (or lit m^{-2} h^{-1}) for the grass, 10.8 mm h^{-1} for the shrubs and 11.4 mm h^{-1} for the dry bare soil.

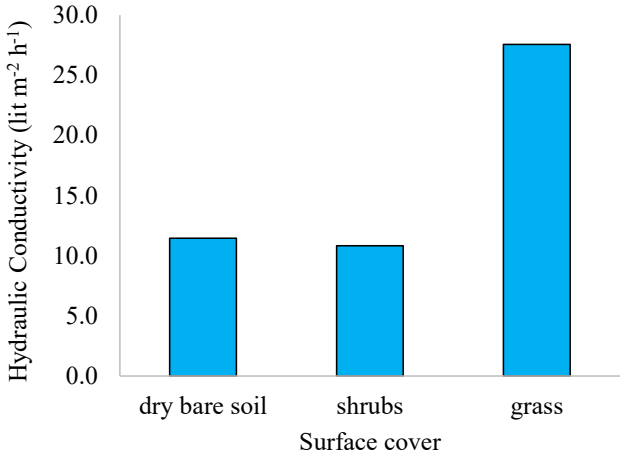

Figure 6. Unsaturated hydraulic conductivity values for soils with a different cover in the UGS.

Hidayat et al. [44] found that soil characteristics, including hydraulic conductivity, are affected by the forest canopy cover, with higher hydraulic conductivity at high-density canopies. The similar values for the bare soil and the shrubs in our UGS are probably attributed to the fact that the shrub-covered surface was only recently (1 year ago) planted and, thus, the short time slot passed was not enough to allow both the soil and the plants root to formulate water paths in the soil to enhance infiltration.

Vegetation improves the soil structure and increases the soil's unsaturated conductivity. However, the time passing after the vegetation installation is critical. In a previous work by Galli et al. [54] on UGSs, the authors found increased unsaturated hydraulic conductivity values in rehabilitated soils, especially five years after the soil rehabilitation. They also identified that unsaturated hydraulic conductivity may decrease after 9–12 years in UGSs with no soil and vegetation maintenance. In our study, the soil at the spaces where shrubs were planted, was only maintained at the specific spots where the plants were established, whereas the experiments for the determination of the unsaturated hydraulic conductivity were conducted between the spots, where there was no soil maintenance.

On the other hand, the grass sections of the UGS were the only ones frequently irrigated and maintained, and within the first year of the grass installation, a dense root system was formulated and enhanced the soil's ability to infiltrate water. Galli et al. [54] identified the time after soil rehabilitation, the soil compaction and the vegetation cover as the most critical factors affecting the unsaturated hydraulic conductivity in the UGSs. They

suggested that the higher unsaturated hydraulic conductivity values in the examined rehabilitated green spaces were associated with the time after the vegetation introduction. This is due to the fact that as the plants grow their root system, the development of a coherent soil matrix with stable connections between pores and the establishment of pathways for the water movement inside the soil, are enhanced. In addition, many studies [46,49–51] support that soil hydraulic conductivity is highly affected by the growth of the plant's roots, and this is accredited to water's preferential flow around the roots [52].

4. Conclusions

The positive impact of Urban Green Spaces (UGS) on the local climate is generally accepted, imposing a need to redesign our cities by enhancing green infrastructure in order to cope with climate change and establish resilient cities and neighborhoods. The positive effect of UGSs is attributed to their micrometeorological–optical characteristics and hydraulics properties that allow for the greater absorbance of solar radiation without increasing stored heat in the urban environment and, also, the increased water infiltration, which, in large scales, can reduce flooding phenomena.

In the present study, we present the findings of a campaign implemented in an UGS in Amaroussion city in Athens—Greece, where solar reflectance (albedo) and surface temperatures were measured above the different-type surfaces of the UGS during the midday of a warm summer day (23 June 2022), using portable radiometers and infrared thermometers. In addition, the soil hydraulic conductivity was estimated for bare soil and vegetation-covered surfaces in the UGS.

The results show that natural surfaces have lower reflection coefficients (0.14 for grass and shrub-covered surfaces and 0.15 for dry bare soil) compared to the artificial ones (albedo values 0.27 for concrete, 0.21 for asphalt and 0.20 for paved-covered surfaces). The surface temperatures of the natural elements are also cooler compared to the surrounding air (direct air temperatures measured above the surfaces with unshielded thermometers) presenting higher negative differences above vegetation –5.5 °C (for shrubs) and –3.8 °C (grass). The bare dry soil and the artificial surfaces are much warmer presenting positive surface to direct air temperature differences, with values of +7.8 °C (+8.7 °C) for the paved surfaces inside (outside of) the UGS, +10.8 °C for the dry bare soil, +12.2 °C for concrete and +12.5 °C for asphalt-covered surfaces. The above findings indicate that the vegetation-covered surfaces absorb higher solar radiation quantities that, however, do not lead to increases in the surfaces' temperatures. On the other hand, the artificial element's optical behavior allows higher radiation reflectance, and the absorbed solar radiation fluxes lead to higher surface temperatures enhancing the urban heat island effect.

The hydraulic conductivity of the unsaturated soil is higher at the grass-covered surfaces and less at dry bare soils and shrub-covered surfaces inside the UGS, indicating faster infiltration of the precipitation water, which is very important when assessing the performance of UGSs to prevent urban floods.

The above results refer to the micrometeorological attributes of a small urban green area, during the noon of a very warm summer day with clear sky conditions and high incoming radiation fluxes. The temporal (diurnal or seasonal) changes of the atmospheric environment are also important to be studied, in order to understand the behavior of the urban green infrastructures and their impact on formatting the urban climate. Additional sites inside the urban environment, especially in the Mediterranean, should also be studied to reach sound conclusions.

The study of additional urban green areas in the broader area of Athens, with different materials and green species composition and in different seasons are within the future research goals of the researchers of this work, in order to verify and quantify the micrometeorological characteristics of urban green areas and their effect on the Mediterranean urban climate.

Author Contributions: Conceptualization, N.D.P.; methodology, N.D.P. and A.D.S.; software, N.D.P.; validation, N.D.P. and M.P.; formal analysis, N.D.P., A.D.S., and N.E.C.; investigation, N.D.P., A.D.S., M.P., and N.E.C.; resources, N.D.P. and M.P.; data curation, N.D.P.; writing—original draft preparation, N.D.P., A.D.S., and M.P.; writing—review and editing, N.D.P., A.D.S., M.P., and N.E.C.; visualization, N.D.P.; supervision, N.D.P. All authors have read and agreed to the published version of the manuscript.

Funding: This research was funded by the LIFE GrIn project "Promoting urban Integration of GReen INfrastructure to improve climate governance in cities" LIFE17 GIC/GR/000029, which is co-funded by the European Commission under the Climate Change Action-Climate Change Governance and Information component of the LIFE Programme and the Greek Green Fund.

Data Availability Statement: The data presented in this study are available on request from the corresponding author.

Acknowledgments: The authors highly acknowledge the contribution of Nikolaos Papaioannou, for providing the June 2022 meteorological data from the automatic meteorological station of the Municipality of Amaroussion—Greece, installed on the roof of the 5th Elementary School of Amaroussion.

Conflicts of Interest: The authors declare no conflict of interest.

References

1. Kolimenakis, A.; Solomou, A.D.; Proutsos, N.; Avramidou, E.V.; Korakaki, E.; Karetsos, G.; Maroulis, G.; Papagiannis, E.; Tsagkari, K. The socioeconomic welfare of urban green areas and parks; a literature review of available evidence. *Sustainability* **2021**, *13*, 7863. https://doi.org/10.3390/su13147863.
2. Kolimenakis, A.S.; Proutsos, N.D.; Avramidou, E.V.; Korakaki, E.; Karetsos, G.; Kontogianni, A.B.; Kontos, K.; Georgiadis, Ch.; Maroulis, G.; Papagiannis, E.; et al. The socioeconomic importance of Urban Green Areas in the era of COVID-19: A case study of nationwide survey in Greece. *Land* **2022**, *submitted paper-under revision*.
3. Cao, X.; Onishi, A.; Chen, J.; Imura, H. Quantifying the cool island intensity of urban parks using ASTER and IKONOS data. *Landsc. Urban Plan.* **2010**, *96*, 224–231. https://doi.org/10.1016/j.landurbplan.2010.03.008.
4. Chen, X.-L.; Zhao, H.-M.; Li, P.-X.; Yin, Z.-Y. Remote sensing image-based analysis of the relationship between urban heat island and land use/cover changes. *Remote Sens. Environ.* **2006**, *104*, 133–146. https://doi.org/10.1016/j.rse.2005.11.016.
5. Tran, H.; Uchihama, D.; Ochi, S.; Yasuoka, Y. Assessment with satellite data of the urban heat island effects in Asian mega cities. *Int. J. Appl. Earth Obs. Geoinf.* **2006**, *8*, 34–48. https://doi.org/10.1016/j.jag.2005.05.003.
6. Voogt, J.A.; Oke, T. Effects of urban surface geometry on remotely-sensed surface temperature. *Int. J. Remote Sens.* **1998**, *19*, 895–920. https://doi.org/10.1080/014311698215784.
7. Weng, Q. Thermal infrared remote sensing for urban climate and environmental studies: Methods, applications, and trends. *ISPRS J. Photogramm. Remote Sens.* **2009**, *64*, 335–344. https://doi.org/10.1016/j.isprsjprs.2009.03.007.
8. Weng, Q.; Lu, D.; Schubring, J. Estimation of land surface temperature–vegetation abundance relationship for urban heat island studies. *Remote Sens. Environ.* **2004**, *89*, 467–483. https://doi.org/10.1016/j.rse.2003.11.005.
9. Qiu, G.Y.; Zou, Z.; Li, X.; Li, H.; Guo, Q.; Yan, C.; Tan, S. Experimental studies on the effects of green space and evapotranspiration on urban heat island in a subtropical megacity in China. *Habitat Int.* **2017**, *68*, 30–42. https://doi.org/10.1016/j.habitatint.2017.07.009.
10. Maimaitiyiming, M.; Ghulam, A.; Tiyip, T.; Pla, F.; Latorre-Carmona, P.; Halik, Ü.; Sawut, M.; Caetano, M. Effects of green space spatial pattern on land surface temperature: Implications for sustainable urban planning and climate change adaptation. *ISPRS J. Photogramm. Remote Sens.* **2014**, *89*, 59–66. https://doi.org/10.1016/j.isprsjprs.2013.12.010.
11. Li, X.; Zhou, W.; Ouyang, Z.; Xu, W.; Zheng, H. Spatial pattern of greenspace affects land surface temperature: Evidence from the heavily urbanized Beijing metropolitan area, China. *Landsc. Ecol.* **2012**, *27*, 887–898. https://doi.org/10.1007/s10980-012-9731-6.
12. Zhang, X.; Zhong, T.; Feng, X.; Wang, K. Estimation of the relationship between vegetation patches and urban land surface temperature with remote sensing. *Int. J. Remote Sens.* **2009**, *30*, 2105–2118. https://doi.org/10.1080/01431160802549252.
13. Qiu, G.-Y.; LI, H.-Y.; Zhang, Q.-T.; Wan, C.; Liang, X.-J.; Li, X.-Z. Effects of evapotranspiration on mitigation of urban temperature by vegetation and urban agriculture. *J. Integr. Agric.* **2013**, *12*, 1307–1315. https://doi.org/10.1016/S2095-3119(13)60543-2.
14. Mackey, C.W.; Lee, X.; Smith, R.B. Remotely sensing the cooling effects of city scale efforts to reduce urban heat island. *Building and Environment*, **2012**, 49, 348-358. https://doi.org/10.1016/j.buildenv.2011.08.004.
15. Jusuf, S.K.; Wong, N.H.; Hagen, E.; Anggoro, R.; Hong, Y. The influence of land use on the urban heat island in Singapore. *Habitat Int.* **2007**, *31*, 232–242. https://doi.org/10.1016/j.habitatint.2007.02.006.
16. Huang, M.; Cui, P.; He, X. Study of the cooling effects of urban green space in Harbin in terms of reducing the heat island effect. *Sustainability* **2018**, *10*, 1101. https://doi.org/10.3390/su10041101.

17. Bao, T.; Li, X.; Zhang, J.; Zhang, Y.; Tian, S. Assessing the distribution of urban green spaces and its anisotropic cooling distance on urban heat island pattern in Baotou, China. *ISPRS Int. J. Geo-Inf.* **2016**, *5*, 12. https://doi.org/10.3390/ijgi5020012.
18. Edmondson, J.L.; Stott, I.; Davies, Z.G.; Gaston, K.J.; Leake, J.R. Soil surface temperatures reveal moderation of the urban heat island effect by trees and shrubs. *Sci. Rep.* **2016**, *6*, 33708. https://doi.org/10.1038/srep33708.
19. Armson, D.; Stringer, P.; Ennos, A. The effect of tree shade and grass on surface and globe temperatures in an urban area. *Urban For. Urban Green.* **2012**, *11*, 245–255. https://doi.org/10.1016/j.ufug.2012.05.002.
20. Wu, J.-H.; Tang, C.-S.; Shi, B.; Gao, L.; Jiang, H.-T.; Daniels, J.L. Effect of ground covers on soil temperature in urban and rural areas. *Environ. Eng. Geosci.* **2014**, *20*, 225–237. https://doi.org/10.2113/gseegeosci.20.3.225.
21. Mohajerani, A.; Bakaric, J.; Jeffrey-Bailey, T. The urban heat island effect, its causes, and mitigation, with reference to the thermal properties of asphalt concrete. *J. Environ. Manag.* **2017**, *197*, 522–538. https://doi.org/10.1016/j.jenvman.2017.03.095.
22. Pomerantz, M.; Akbari, H.; Chang, S.-C.; Levinson, R.; Pon, B. Examples of Cooler Reflective Streets for Urban Heat-Island Mitigation: Portland Cement Concrete and Chip Seals. 2003. Available online: https://escholarship.org/content/qt53w2s92d/qt53w2s92d.pdf (accessed on 13 November 2022).
23. Grimmond, S. Urbanization and global environmental change: Local effects of urban warming. *Geogr. J.* **2007**, *173*, 83–88. Available online: https://www.jstor.org/stable/30113496 (accessed on 13 November 2022).
24. Proutsos, N.; Liakatas, A.; Alexandris, S.; Tsiros, I. Carbon fluxes above a deciduous forest in Greece. *Atmósfera* **2017**, *30*, 311–322. https://doi.org/10.20937/atm.2017.30.04.03.
25. Proutsos, N.; Alexandris, S.; Liakatas, A.; Nastos, P.; Tsiros, I.X. PAR and UVA composition of global solar radiation at a high altitude Mediterranean forest site. *Atmos. Res.* **2022**, *269*, 106039. https://doi.org/10.1016/j.atmosres.2022.106039.
26. Proutsos, N.; Liakatas, A.; Alexandris, S. Ratio of photosynthetically active to total incoming radiation above a Mediterranean deciduous oak forest. *Theor. Appl. Climatol.* **2019**, *137*, 2927–2939. https://doi.org/10.1007/s00704-019-02786-z.
27. Proutsos, N.D.; Liakatas, A.; Alexandris, S.G.; Tsiros, I.X.; Tigkas, D.; Halivopoulos, G. Atmospheric Factors Affecting Global Solar and Photosynthetically Active Radiation Relationship in a Mediterranean Forest Site. *Atmosphere* **2022**, *13*, 1207. https://doi.org/10.3390/atmos13081207.
28. Liakatas, A.; Proutsos, N.; Alexandris, S. Optical properties affecting the radiant energy of an oak forest. *Meteorol. Appl.* **2002**, *9*, 433–436. https://doi.org/10.1017/S135048270200405X.
29. Baldinelli, G.; Bonafoni, S.; Rotili, A. Albedo retrieval from multispectral landsat 8 observation in urban environment: Algorithm validation by in situ measurements. *IEEE J. Sel. Top. Appl. Earth Obs. Remote Sens.* **2017**, *10*, 4504–4511. https://doi.org/10.1109/JSTARS.2017.2721549.
30. Jin, M.S.; Kessomkiat, W.; Pereira, G. Satellite-observed urbanization characters in Shanghai, China: Aerosols, urban heat island effect, and land–atmosphere interactions. *Remote Sens.* **2011**, *3*, 83–99. https://doi.org/10.3390/rs3010083.
31. Kjelgren, R.; Montague, T. Urban tree transpiration over turf and asphalt surfaces. *Atmos. Environ.* **1998**, *32*, 35–41. https://doi.org/10.1016/S1352-2310(97)00177-5.
32. Debbage, N.; Shepherd, J.M. The urban heat island effect and city contiguity. *Comput. Environ. Urban Syst.* **2015**, *54*, 181–194. https://doi.org/10.1016/j.compenvurbsys.2015.08.002.
33. Chudnovsky, A.; Ben-Dor, E.; Saaroni, H. Diurnal thermal behavior of selected urban objects using remote sensing measurements. *Energy Build.* **2004**, *36*, 1063–1074. https://doi.org/10.1016/j.enbuild.2004.01.052.
34. Kalnay, E.; Cai, M. Impact of urbanization and land-use change on climate. *Nature* **2003**, *423*, 528–531. https://doi.org/10.1038/nature01675.
35. Kalnay, E.; Cai, M. Correction: Corrigendum: Impact of urbanization and land-use change on climate. *Nature* **2003**, *425*, 102–102. https://doi.org/10.1038/nature01952.
36. Erell, E.; Pearlmutter, D.; Boneh, D.; Kutiel, P.B. Effect of high-albedo materials on pedestrian heat stress in urban street canyons. *Urban Clim.* **2014**, *10*, 367–386. https://doi.org/10.1016/j.uclim.2013.10.005.
37. Giannopoulou, K.; Livada, I.; Santamouris, M.; Saliari, M.; Assimakopoulos, M.; Caouris, Y. On the characteristics of the summer urban heat island in Athens, Greece. *Sustain. Cities Soc.* **2011**, *1*, 16–28. https://doi.org/10.1016/j.scs.2010.08.003.
38. Livada, I.; Santamouris, M.; Niachou, K.; Papanikolaou, N.; Mihalakakou, G. Determination of places in the great Athens area where the heat island effect is observed. *Theor. Appl. Climatol.* **2002**, *71*, 219–230. https://doi.org/10.1007/s007040200006.
39. Skoulika, F.; Santamouris, M.; Kolokotsa, D.; Boemi, N. On the thermal characteristics and the mitigation potential of a medium size urban park in Athens, Greece. *Landsc. Urban Plan.* **2014**, *123*, 73–86. https://doi.org/10.1016/j.landurbplan.2013.11.002.
40. Zoulia, I.; Santamouris, M.; Dimoudi, A. Monitoring the effect of urban green areas on the heat island in Athens. *Environ. Monit. Assess.* **2009**, *156*, 275–292. https://doi.org/10.1007/s10661-008-0483-3.
41. Melas, E.; Tsiros, I.; Thoma, E.; Proutsos, N.; Pantavou, K.; Papadopoulos, G. An assessment of microclimatic conditions inside vegetated and non-vegetated small-scale open spaces in the Athens urban environment. In Proceedings of the 15th International Conference on Meteorology, Climatology and Atmospheric Physics—COMECAP 2021, Ioannina, Greece, 26–29 September 2021; pp. 269–273.
42. Tsiros, I.X.; Hoffman, M.E. Thermal and comfort conditions in a semi-closed rear wooded garden and its adjacent semi-open spaces in a Mediterranean climate (Athens) during summer. *Archit. Sci. Rev.* **2014**, *57*, 63–82. https://doi.org/10.1080/00038628.2013.829021.
43. Tsiros, I.X. Assessment and energy implications of street air temperature cooling by shade tress in Athens (Greece) under extremely hot weather conditions. *Renew. Energy* **2010**, *35*, 1866–1869. https://doi.org/10.1016/j.renene.2009.12.021.

44. Hidayat, Y.; Purwakusuma, W.; Wahjunie, E.D.; Baskoro, D.P.T.; Rachman, L.M.; Yusuf, S.M.; Adawiyah, R.M.; Syaepudin, I.; Siregar, M.M.R.; Isnaini, D.A. Characteristics of soil hydraulic conductivity in natural forest, agricultural land, and green open space area. *J. Pengelolaan Sumberd. Alam Dan Lingkung. J. Nat. Resour. Environ. Manag.* **2022**, *12*, 352–362. https://doi.org/10.29244/jpsl.12.2.352-362.
45. Luo, W.; Li, J.; Song, L.; Cheng, P.; Garg, A.; Zhang, L. Effects of vegetation on the hydraulic properties of soil covers: Four-years field experiments in Southern China. *Rhizosphere* **2020**, *16*, 100272. https://doi.org/10.1016/j.rhisph.2020.100272.
46. Gadi, V.K.; Tang, Y.-R.; Das, A.; Monga, C.; Garg, A.; Berretta, C.; Sahoo, L. Spatial and temporal variation of hydraulic conductivity and vegetation growth in green infrastructures using infiltrometer and visual technique. *Catena* **2017**, *155*, 20–29. https://doi.org/10.1016/j.catena.2017.02.024.
47. Garg, A.; Leung, A.K.; Ng, C.W.W. Comparisons of soil suction induced by evapotranspiration and transpiration of *S. heptaphylla*. *Can. Geotech. J.* **2015**, *52*, 2149–2155. https://doi.org/10.1139/cgj-2014-0425.
48. Leung, A.K.; Garg, A.; Coo, J.L.; Ng, C.W.W.; Hau, B. Effects of the roots of Cynodon dactylon and Schefflera heptaphylla on water infiltration rate and soil hydraulic conductivity. *Hydrol. Process.* **2015**, *29*, 3342–3354. https://doi.org/10.1002/hyp.10452.
49. Ghestem, M.; Sidle, R.C.; Stokes, A. The influence of plant root systems on subsurface flow: Implications for slope stability. *Bioscience* **2011**, *61*, 869–879. https://doi.org/10.1525/bio.2011.61.11.6.
50. Mitchell, A.; Ellsworth, T.; Meek, B. Effect of root systems on preferential flow in swelling soil. *Commun. Soil Sci. Plant Anal.* **1995**, *26*, 2655–2666. https://doi.org/10.1080/00103629509369475.
51. Noordwijk, M.V.; Heinen, M.; Hairiah, K. Old tree root channels in acid soils in the humid tropics: Important for crop root penetration, water infiltration and nitrogen management. In *Plant-Soil Interactions at Low pH*; Springer: Berlin/Heidelberg, Germany, 1991; pp. 423–430.
52. Nieber, J.L.; Sidle, R.C. How do disconnected macropores in sloping soils facilitate preferential flow? *Hydrol. Process.* **2010**, *24*, 1582–1594. https://doi.org/10.1002/hyp.7633.
53. Jarvis, N.; Koestel, J.; Messing, I.; Moeys, J.; Lindahl, A. Influence of soil, land use and climatic factors on the hydraulic conductivity of soil. *Hydrol. Earth Syst. Sci.* **2013**, *17*, 5185–5195. https://doi.org/10.5194/hess-17-5185-2013.
54. Galli, A.; Peruzzi, C.; Beltrame, L.; Cislaghi, A.; Masseroni, D. Evaluating the infiltration capacity of degraded vs. rehabilitated urban greenspaces: Lessons learnt from a real-world Italian case study. *Sci. Total Environ.* **2021**, *787*, 147612. https://doi.org/10.1016/j.scitotenv.2021.147612.
55. Arnold, E. *World Atlas of Desertification*; UNEP: London, UK, 1992.
56. Thornthwaite, C. Una aproximación para una clasificación racional del clima. *Geogr. Rev.* **1948**, *38*, 85–94. https://doi.org/10.2307/210739.
57. Thornthwaite, C.W.J.; Mather, J.R. *The Water Balance Climatology*; Drexel Institute of Technology, Laboratory of Climatology: Centerton, New Jersey, USA, 1955.
58. Proutsos, N.D.; Tsiros, I.X.; Nastos, P.; Tsaousidis, A. A note on some uncertainties associated with Thornthwaite's aridity index introduced by using different potential evapotranspiration methods. *Atmos. Res.* **2021**, *260*, 105727. https://doi.org/10.1016/j.atmosres.2021.105727.
59. Tsiros, I.X.; Nastos, P.; Proutsos, N.D.; Tsaousidis, A. Variability of the aridity index and related drought parameters in Greece using climatological data over the last century (1900–1997). *Atmos. Res.* **2020**, *240*, 104914.
60. Proutsos, N.D.S.; Tigkas, D.A. Decadal variation of aridity and water balance attributes at the urban and peri-urban environment of Attica-Greece. In Proceedings of the HAICTA 2022: 10th International Conference on ICT in Agriculture, Food & Environment, Athens, Greece, 22–25 September 2022.
61. Alexandris, S.; Proutsos, N. How significant is the effect of the surface characteristics on the Reference Evapotranspiration estimates? *Agric. Water Manag.* **2020**, *237*, 106181. https://doi.org/10.1016/j.agwat.2020.106181.
62. Zhang, R. Determination of soil sorptivity and hydraulic conductivity from the disk infiltrometer. *Soil Sci. Soc. Am. J.* **1997**, *61*, 1024–1030. https://doi.org/10.2136/sssaj1997.03615995006100040005x.
63. Carsel, R.F.; Parrish, R.S. Developing joint probability distributions of soil water retention characteristics. *Water Resour. Res.* **1988**, *24*, 755–769. https://doi.org/10.1029/WR024i005p00755.
64. Golden Software LLC. Surfer®® ver. 13. Available online: https://www.goldensoftware.com/products/surfer (accessed on 7 November 2022).
65. Salvati, L.; Zitti, M.; Di Bartolomei, R.; Perini, L. Climate aridity under changing conditions and implications for the agricultural sector: Italy as a case study. *Geogr. J.* **2012**, *2013*, 923173. https://doi.org/10.1155/2013/923173.
66. Ha, J.; Lee, S.; Park, C. Temporal effects of environmental characteristics on urban air temperature: The influence of the sky view factor. *Sustainability* **2016**, *8*, 895. https://doi.org/10.3390/su8090895.
67. Jaganmohan, M.; Knapp, S.; Buchmann, C.M.; Schwarz, N. The bigger, the better? The influence of urban green space design on cooling effects for residential areas. *J. Environ. Qual.* **2016**, *45*, 134–145. https://doi.org/10.2134/jeq2015.01.0062.
68. Monteiro, M.V.; Doick, K.J.; Handley, P.; Peace, A. The impact of greenspace size on the extent of local nocturnal air temperature cooling in London. *Urban For. Urban Green.* **2016**, *16*, 160–169. https://doi.org/10.1016/j.ufug.2016.02.008.
69. Ca, V.T.; Asaeda, T.; Abu, E.M. Reductions in air conditioning energy caused by a nearby park. *Energy Build.* **1998**, *29*, 83–92. https://doi.org/10.1016/S0378-7788(98)00032-2.
70. Tong, H.; Walton, A.; Sang, J.; Chan, J.C. Numerical simulation of the urban boundary layer over the complex terrain of Hong Kong. *Atmos. Environ.* **2005**, *39*, 3549–3563. https://doi.org/10.1016/j.atmosenv.2005.02.045.

71. Yu, C.; Hien, W.N. Thermal benefits of city parks. *Energy Build.* **2006**, *38*, 105–120. https://doi.org/10.1016/j.enbuild.2005.04.003.
72. Đekić, J.P.; Mitković, P.B.; Dinić-Branković, M.M.; Igić, M.Z.; Đekić, P.S.; Mitković, M.P. The study of effects of greenery on temperature reduction in urban areas. *Therm. Sci.* **2018**, *22*, 988–1000. https://doi.org/10.2298/TSCI170530122D.
73. Oke, T.R. *Boundary Layer Climates*, 2nd ed.; Routledge: 1987; pp. 464. https://doi.org/10.4324/9780203407219.
74. Aida, M. Urban albedo as a function of the urban structure—A model experiment. *Bound. -Layer Meteorol.* **1982**, *23*, 405–413. https://doi.org/10.1007/BF00116269.
75. Sugawara, H.; Takamura, T. Surface albedo in cities: Case study in Sapporo and Tokyo, Japan. *Bound. -Layer Meteorol.* **2014**, *153*, 539–553. https://doi.org/10.1007/s10546-014-9952-0.